

Models for estimating the leaf NDVI of japonica rice on a canopy scale by combining canopy NDVI and multisource environmental data in Northeast China

Yu Fenghua¹, Xu Tongyu^{1*}, Cao Yingli¹, Yang Guijun², Du Wen¹, Wang Shu³

(1. College of Information and Electrical Engineering, Shenyang Agricultural University, Shenyang 110866, China;

2. Beijing Research Center for Information Technology in Agriculture, Beijing 100097, China;

3. College of Agronomy, Shenyang Agricultural University, Shenyang 110866, China)

Abstract: Remote sensing of rice traits has advanced significantly with regard to the capacity to retrieve useful plant biochemical, physiological and structural quantities across spatial scales. The rice leaf NDVI (normalized difference vegetation index) has been developed and applied in monitoring rice growth, yield prediction and disease status to guide agricultural management practices. This study combined rice canopy NDVI and environmental data to estimate rice leaf NDVI. The test site was a japonica rice experiment located in the eastern city of Shenyang, Liaoning Province, China. This paper describes (1) the use of multiple linear regression to establish four periods of rice leaf NDVI models with good accuracy ($R^2=0.782-0.903$), and (2) how the key point of the rice growth period based on these models was determined. The techniques for modeling leaf NDVI at the point of remote canopy sensing were also presented. The results indicate that the rice leaf NDVI has a high correlation with the canopy NDVI and multisource environmental data. This research can provide an efficient method to detect rice leaf growth at the canopy scale in the future.

Keywords: japonica rice, NDVI, leaf models, canopy scale, environmental data

DOI: 10.3965/j.ijabe.20160905.2266

Citation: Yu F H, Xu T Y, Cao Y L, Yang G J, Du W, Wang S. Models for estimating the leaf NDVI of japonica rice on a canopy scale by combining canopy NDVI and multisource environmental data in Northeast China. *Int J Agric & Biol Eng*, 2016; 9(5): 132–142.

1 Introduction

China has the second largest rice-planting area in the world and the largest annual rice output (204 million tons). Rice cultivation in northeast China is based mainly on japonica rice, for which the planting area accounts for

more than 30% of the total rice area and continues to increase^[1].

The leaf of the rice plant constitutes its photosynthetic vegetative organ, the total nitrogen concentration with regard to nutrition being an important indicator for diagnosis. Traditional nitrogen-monitoring methods for rice generally rely on field-sampling of plants in the field and subsequent indoor testing. Although the results from such testing are more reliable, the temporal and spatial scales present difficulties in meeting real-time, rapid, non-destructive diagnoses of nitrogen requirements. With the development of modern remote sensing technology, this technology has included an estimation of the chemical composition of nitrogen when applied to rice. In theory and practice for the evaluation of rice

Received date: 2015-12-11 **Accepted date:** 2016-05-23

Biographies: Yu Fenghua, PhD Candidate, research interest: agricultural remote sensing, Email: adan@syau.edu.cn; Cao Yingli, PhD, Associate Professor, research interest: agricultural remote sensing, Email: 24223732@qq.com; Yang Guijun, PhD, research professorship, research interest: agricultural remote sensing, Email: yanggj@nercita.org.cn; Du Wen, PhD Candidate, research interest: agricultural remote sensing, Email: duwen@syau.edu.cn; Wang Shu, PhD, Professor, research interest: crop cultivation and farming system, Email: wangshu1@126.com.

***Corresponding author:** Xu Tongyu, PhD, Professor, research interest: agricultural remote sensing, Email: yatongmu@163.com.

growth and its physiological parameters, remote sensing can guarantee reliable outcomes.

Applying remote sensing technology to obtain information on rice growth has been rapidly developed in recent years because of its low cost, nondestructive testing processes, and other wide-ranging advantages^[2]. The different characteristics of the spectral data on rice constitute the theoretical basis for using remote sensing technology to obtain information on growth through spectral analytical methods to identify and extract the corresponding phenotypic traits and spectral vegetation indices (VIs). The VIs can reduce the influence of external factors to a certain extent and thus enhance rice-growth information^[3].

In 1999, a group of investigators funded by the NASA Earth Observations Commercialization and Applications Program (EOCAP) pooled their resources to conduct a nitrogen fertilization experiment aiming to prove that agricultural crops must undergo dry-matter accumulation during photosynthesis of chlorophyll in their leaves^[4]. Therefore, leaves need a lot of red and blue light to complete the process of photosynthesis. As rice is growing, it exhibits a strong absorption phenomenon in the visible region (VR) of sunlight radiation and weak absorption in the near infrared region (NIR) of sunlight^[5]. The spectral bands used by most VIs are concentrated in the VR-to-NIR (350-1700 nm) range. At present, the VIs of phenotypic traits in rice consist of more than 50 species, such as the ratio vegetation index (RVI), the normalized difference vegetation index (NDVI), the soil-regulation vegetation index (SAVI), the difference vegetation index (DVI), and the enhanced vegetation index (EVI)^[6,7]. Some research has shown good NDVI data for crop production and biomass estimation^[8-11]. However, the NDVI does not reflect rice growth in the internal mechanism process. Although many agronomists and rice NDVI parameters have been considered, their models are based mostly on the establishment of statistical methods for remote sensing estimates, frequently with relatively strong empirical models and relatively poor versatility^[12-14]. The general remote-sensing method to obtain a rice canopy NDVI takes advantage of natural light; therefore, the acquired

NDVI is affected by light conditions, the atmosphere, and aerosols, all of which contribute to reduced accuracy. In Northeast China, the variety of rice known as japonica (Shendao-47, Shendao-525, etc.) consists vertical leaves mainly. A canopy NDVI can also be affected by soil, water layers, green algae, and other surface features, all of which act as interfering factors that greatly influence the accuracy of the NDVI in a rice canopy.

The objective of this study was to use rice canopy NDVI and environmental data to model rice leaf NDVI. The researchers collected different scales of NDVI data (from both canopy and leaves) from the Shenyang Agricultural University experimental rice-breeding fields. The data were acquired during the rice-cultivation period from transplanting to maturity (June 2015-October 2015). The leaf NDVI model of northeast japonica rice was based on remote fusion sensing and environmental factors such as temperature and humidity during the number of growing days, sunlight hours, and rice-growing microenvironments^[15].

2 Materials and methods

2.1 Testing site

The testing site was an experimental rice-breeding field at Shenyang Agricultural University (41°49'N, 123°33'E; altitude 65 m) in Shenyang, Liaoning Province, China.

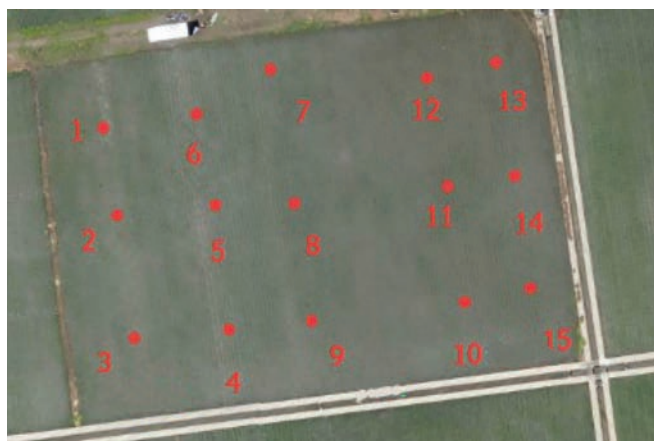
The japonica rice (Shendao-47) cultivar was transplanted on May 28, 2015.

The typical properties of Shendao-47 include the following:

- 1) compactness;
- 2) robust seedlings;
- 3) strong tillering features;
- 4) erect leaves;
- 5) yellow glumes and tips;
- 6) semi-erect panicles, numbering about 1.2 to 1.5 million per acre;
- 7) 160 flowers and 140-200 grains per panicle;
- 8) 25-cm ear lengths;
- 9) heights of about 105 cm;
- 10) about 90% granulation;
- 11) 350-400 m² planting areas.

China has 10 indicators to meet its high-quality, high-palatability rice standard. Some varieties are resistant to blasts, lodging, low temperatures, and drought (for the medium-ripe variety). Shendao-47 is widely cultivated in Shenyang, where the growth period is 155-156 d. Other areas of widespread cultivation include Liaoyang, Anshan, Yingkou, Panjin, and North China^[16-18].

NDVI data were collected from both leaf and canopy in an area of 0.5 m². The average sets had 15 sampling points for testing in a paddy field, as illustrated in Figure 1. The instruments used were a Plant-Pen NDVI-300 (PSI Corporation, Czech Republic) for the leaf NDVI data collection and a SpectroSense2+ (Skye Corporation, UK) for the canopy NDVI data collection^[19-22]. Temperature and humidity data were collected by using a wireless sensor network^[23]. The sensors were distributed inside the plots (at points 1-9) and 2 m above the rice fields at each temperature. The humidity collection point heights were divided into three sections: the bottom of rice growth (10 cm), mid-area growth (60 cm), and the canopy (110 cm). The-growth data were collected at different heights, micro-environmental temperatures, and humidity levels.



Note: points 1-15 designate sampling area; Background: Shendao-47, June 17, 2015, UAV collection.

Figure 1 Test site: japonica rice experiment at Shenyang Agricultural University in 2015

2.2 NDVI data collection

2.2.1 Leaf NDVI

Rice leaf NDVI data were collected by using a PlantPen NDVI-300 as the active light source for the measuring instrument. The center of the visible-light wavelength of the instrument was 660 nm (VIS=660 nm); the near-infrared light-source center wavelength, 740 nm

(NIR=740 nm); and the range, 620-750 nm^[24]. The leaf NDVI measurement period was from a week after transplanting (June 4) to harvesting (October 1). The time for measurement was 10:30–13:30 daily. On rainy days measurement was postponed until the rain ended, but not later than 16:00. Given the relative slenderness of north japonica rice leaves, this study included pointed and three-tail leaves, as measured by three NDVI data sets averaged as single-leaf NDVI values. For each sample, the number of leaves collected was considered as an NDVI point for the entire canopy sampling area (0.5 m²), the area of leaves, and the resulting calculated average. The leaf NDVI for the region was then obtained. For rice in the tillering stage of rapid growth, the sampling points in the region included many leaves to ensure accurate data. The rice canopy leaves and rice fields within the main leaf angle blade were averaged for the entire sampling area to obtain the average NDVI value of the leaves (not less than 70 leaves).

2.2.2 Canopy NDVI

Rice canopy NDVI data were very important in this study, for which the canopy-measuring instrument used was a SpectroSense2+ (Figure 2a), which has a passive light source. The corresponding wavelength of the solar radiation incident intensity was measured, and the vegetation canopy of the reflected light was set to be strong on the basis of the measurement of the corresponding spectral characteristics^[25]. To reduce the error caused by the different spectral bands, the selected sensor band was kept consistent with the measurement range of the Plant-Pen NDVI-300 (Figure 2b), the detection range was 620-750 nm. The canopy NDVI measurement time was consistent with the leaf NDVI. Moreover, to reduce human error during the canopy NDVI measurement process, steps were taken to ensure that the backs of the personnel and the instruments were not measured in the coverage area (Figure 2c).

2.3 Measurement of field environmental parameters

The NDVI does not represent a physical quantity of rice; thus, the models of NDVI and rice growth show an unclear growth mechanism. Such models cannot clarify the underlying mechanism of change and its relationship with the NDVI^[26,27]. Under a same-soil condition, the growth of rice is mainly affected by environmental factors.



a. SpectroSense2+ for canopy NDVI collection

b. NDVI-300, for leaf NDVI collection

c. canopy NDVI measurements

Note: Center of visible-light wavelength of instrument, 660 nm (R=660 nm); near-infrared light-source center wavelength, 740 nm (NIR=740 nm).

Figure 2 Testing instruments

In this study, fifteen wireless temperature and humidity sensor networks were set up in the experimental field, each sample was divided into three heights. For each height, temperature and humidity data were obtained in the experimental field, where an external space was also provided with environmental temperature-and-humidity-detection sensors. These wireless sensors communicated through a ZigBee network, the modes of which had star connections. Sensor data (including information such as temperature, humidity, time, and power) were collected every 10 min. The power consumption of the wireless sensor network was low, and the entire experimental process did not require a battery replacement. The sensor used four AAA batteries; the receiver was charged every two days by using solar panels and a mobile power supply to ensure smooth operation of the entire system. Given that the experimental site was located in the northeast region of China, which has rainy days in the summer, the researchers performed waterproof processing for the temperature and humidity tests to ensure that the wireless sensor network is all-weather compatible for temperature and humidity data collection.

2.4 Statistical analyses

Statistical analyses were executed in Microsoft[®] Excel[®] 2013 and IBM[®] SPSS[®] Statistics 22.0.0.0. In accordance with the growth stage of the rice, we analyzed the correlation between the leaf and canopy NDVIs, as well as the respective sunshine-exposure and growth

times of the leaves throughout the entire growth period^[28].

We performed simple linear or exponential regression for leaf and canopy NDVIs, environmental temperature and humidity, as well as respective temperatures and humidity levels within the rice canopy, mid-rice and bottom-rice areas. For day-length data, we used multiple linear regression (MLR)^[29,30]. The following equation was used for the linear model:

$$y_L = \beta_0 + \beta_1 x_C + \beta_2 x_S + \beta_3 x_D + \beta_4 x_{EHH} + \beta_5 x_{ETH} + \beta_6 x_{MTL} + \beta_7 x_{BTL}$$

where, y_L and represent the leaf and canopy NDVIs, respectively; x_S and x_D , the sunshine- and the growth-days of the rice, respectively; x_{EHH} and x_{ETH} , the highest relative humidity levels and temperatures in the environment, respectively; x_{MTL} and x_{BTL} , the lowest temperatures in the middle and bottom parts of the rice, respectively. The model coefficients ($\beta_0, \beta_1, \beta_2, \dots, \beta_7$) were determined for the linear-regression model on the basis of the calibration dataset.

From transplanting to maturity, the growth process of the rice underwent different periods (such as the tillering, jointing, heading, and filling stages), during each of which the changes in the rice leaves and canopy were not the same. Therefore, the different periods in the rice leaf NDVI model should vary^[31]. Accordingly, the leaf NDVI fitting model was divided into four stages: tillering (June), jointing-booting (July), heading and milking (August), and maturity (September) stage models.

3 Results and discussion

3.1 Leaf NDVI modeling

The data collection period for the NDVI fitting model lasted 118 days, from June 4 to September 30. Given that rainy days are unsuitable for NDVI and humidity data collection, the effective number of days was 114. Because the respective durations of the various growth stages of rice are not absolute, we therefore used a monthly modeling process segment, as well as the experimental varieties and planting time in this study, to facilitate future applications of the model^[32]. Moreover, because many of the key growth points were at the beginning or end of a month, the use of segmentation modeling to improve the accuracy of the model was feasible.

We collected the canopy NDVI, sunshine-duration, and micro-environmental growth data for the rice. The linear-regression model was created with SPSS software to obtain the tested paddy-leaf NDVI models for Shendao-47 (Table 1).

Table 1 Shendao-47 leaf NDVI models

Stage	Regression model
Tillering	$y_L = -9.119 + 0.166x_C + 0.633x_S + 0.002x_{EHH}$
Jointing and booting	$y_L = 0.608 - 0.673x_C + 0.051x_S + 0.008x_{MTL} - 0.009x_{BTL}$
Heading to grain-filling	$y_L = 0.965 - 0.285x_C - 0.003x_D + 0.001x_{ETH}$
Maturity	$y_L = -0.705 - 1.056x_C + 0.176x_S - 0.009x_D$

Note: y_L =leaf NDVI, x_C =canopy NDVI, x_S =sunshine, x_D =growth days, x_{EHH} =highest relative humidity, x_{ETH} =highest environmental temperature, x_{MTL} =lowest temperature in bottom part of rice, x_{BTL} =lowest temperature in middle part of rice.

3.2 Model analysis

In this study, the leaf model included the whole rice leaf. The objective of this study was to investigate the effects of environmental factors on the NDVI of the leaves. The experimental area not being very large, the difference of the soil being relatively small, and in order to reduce the complexity of the modeling, the soil condition was considered consistent^[33]. In the process of building the canopy NDVI model as one of the input data, the canopy leaf angle, the effect of water on the soil and other data were input, resulting in a mixed NDVI value.

On the basis of the results listed in Table 2, different-stage leaf models were selected for application

in the model. The dataset was divided into calibration and validation subsets. The validation data consisted of the randomly selected sampling points 1, 5, 9 and 13; whereas, the remaining sampling points served for the calibration. The calibration models (Table 1) were then applied to the validation data and evaluated by the relationship between the observed and the predicted leaf NDVI. The heading-to-grain-filling stage model had a high fit with $R^2=0.845$ and the lowest error ($RMSE=0.092$, $RE=38.36\%$).

Table 2 Coefficient of determination (R^2) and root mean square error (RMSE) for regression between observed and predicted leaf NDVI (RE=relative error)

Stage	R^2	RMSE	RE/%
Tillering	0.845	0.511	48.61
Jointing and booting	0.782	0.131	47.29
Heading to grain-filling	0.877	0.092	38.36
Maturity	0.903	0.235	59.67

3.2.1 Tillering stage

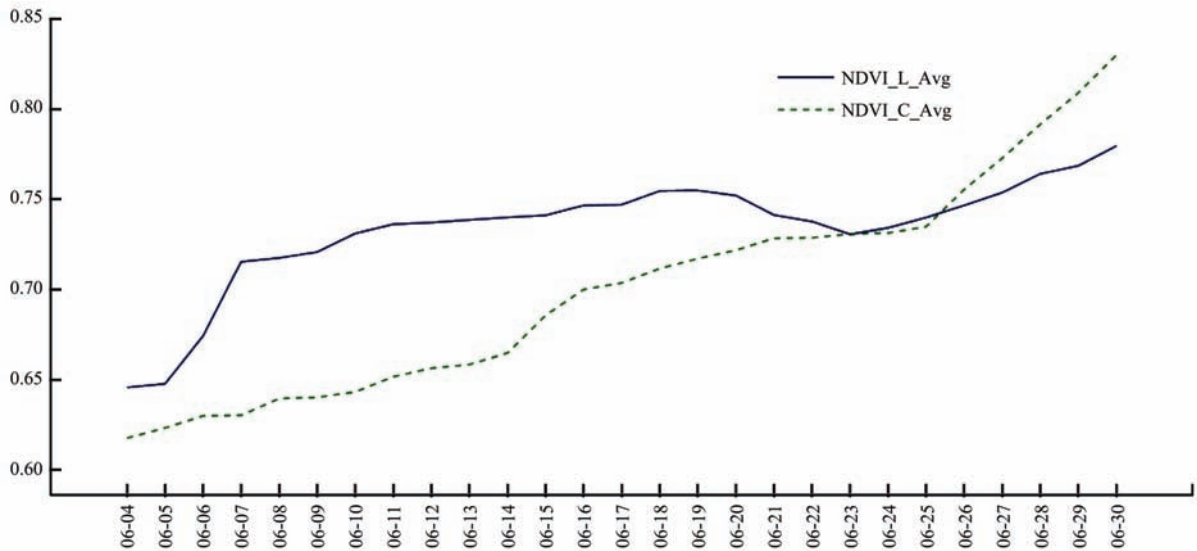
In June, the Shendao-47 was in its tillering stage. The growth of the leaves was related to the maximum relative humidity of the environment and the duration of sunshine. The coefficient of determination R^2 indicated that the maximum relative humidity of the environment for leaf growth had the most obvious effect. This time, the plant height and the leaf area index (LAI) were relatively small^[34]; therefore, the relative humidity at different heights was not obvious. Moreover, the results demonstrated that no significant difference existed between the different models (Table 3).

Table 3 Leaf NDVI modeling and analysis of different environmental parameters in tillering stage

Regression model	R^2
$y_L = -9.119 + 0.166x_C + 0.633x_S + 0.002x_{EHH}$	0.845
$y_L = -7.032 + 0.158x_C + 0.492x_S + 0.002x_{CHH}$	0.839
$y_L = -7.152 + 0.154x_C + 0.5x_S + 0.002x_{MHH}$	0.840
$y_L = -6.461 + 0.179x_C + 0.449x_S + 0.003x_{BHH}$	0.836

Note: y_L =leaf NDVI, x_C =canopy NDVI, x_S =sunshine, x_{EHH} =highest relative humidity in environment, x_{CHH} =highest humidity of canopy rice, x_{MHH} =highest humidity of rice in middle height, x_{BHH} =highest humidity of rice in bottom height.

Figure 3 graphs the time series of the canopy and leaf NDVIs in June. Both NDVIs increased in the tillering stage, but the increase was more obvious in the canopy NDVI. After June 26, the canopy NDVI was greater than the leaf NDVI, this time covering the tillering stage.



Note: NDVI_L_Avg—rice leaf NDVI, NDVI_C_Avg— rice canopy NDVI.

Figure 3 Time-series curves in tillering stage of canopy and leaf NDVIs of Shendao-47 (2015)

3.2.2 Jointing and booting stages

In July, the Shendao-47 was in its jointing and booting stage. The process of achieving accuracy in the NDVI leaf-fitting model was lower than that in other periods mainly because, at this stage, vegetative and reproductive growth ensued. Thus, the process was more complex from the perspective of the model elements. Conversely, for the canopy NDVI, the long-time illumination, the rice-growing environments, as well as the accuracy of the middle-and lower-minimum temperatures of the model were higher than the lowest temperature accuracy of the other model only when actually within the canopy NDVI and in the long-light modeling. Explained at this stage, the vertical-middle and lower-ambient temperatures of the rice had important implications for growth (Table 4).

Table 4 Leaf NDVI modeling and analysis of different environmental parameters in jointing and booting stage

Regression model	R ²
$y_L = 0.542 - 0.664x_C + 0.052x_S$	0.713
$y_L = 0.608 - 0.673x_C + 0.051x_S + 0.008x_{MTL} - 0.009x_{BTL}$	0.782

Note: y_L =leaf NDVI, x_C =canopy NDVI, x_S =sunshine, x_{MTL} =lowest temperature in middle of rice, x_{BTL} =lowest temperature in bottom of rice.

Figure 4 graphs the time series of the canopy and leaf NDVIs in July. Both increased in the tillering stage, but the increase in the canopy NDVI was more obvious. After June 26, the tillering stage, the canopy NDVI was greater than the leaf NDVI. Having relatively stable data, the canopy NDVI was higher than the leaf NDVI;

whereas, the leaf NDVI data decreased because japonica rice growth is complete at tillering. The LAI increased to the maximum value for the entire growth cycle and entered the booting and heading process after the jointing stage. During this period, the ineffective tillers gradually died while, concurrently, some nutritional leaf spikes were gradually transferred^[35].

3.2.3 Grain-filling stage

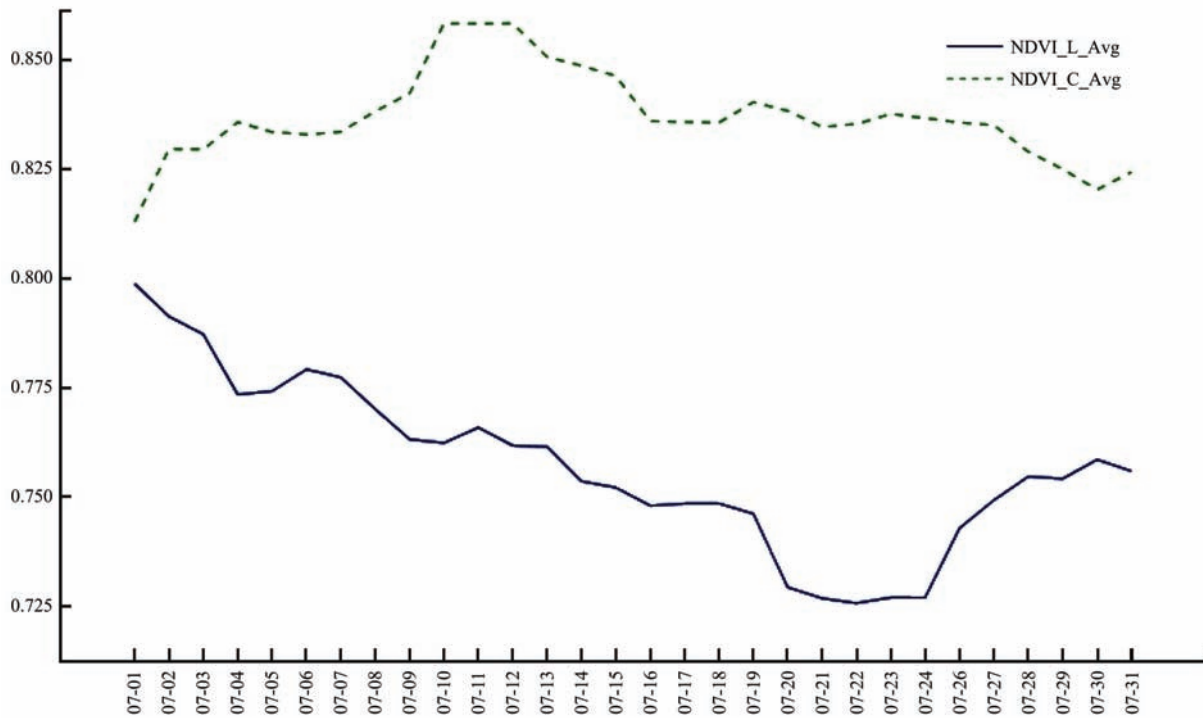
In August, the Shendao-47 was entering the grain-filling reproductive stage. Its growth was affected by the duration of sunshine, the number of growth days, and the changes in temperature within this period. On the basis of the fitting accuracy of the model analysis, the environmental temperature of the height was found to affect the growth (Table 5).

Table 5 Leaf NDVI modeling and analysis of different environmental parameters in grain-filling stage

Regression model	R ²
$y_L = 0.965 - 0.285x_C - 0.003x_D + 0.001x_{ETH}$	0.877
$y_L = 0.942 - 0.262x_C - 0.002x_D + 0.001x_{CTH}$	0.866
$y_L = 0.935 - 0.25x_C - 0.002x_D + 0.001x_{MTH}$	0.861

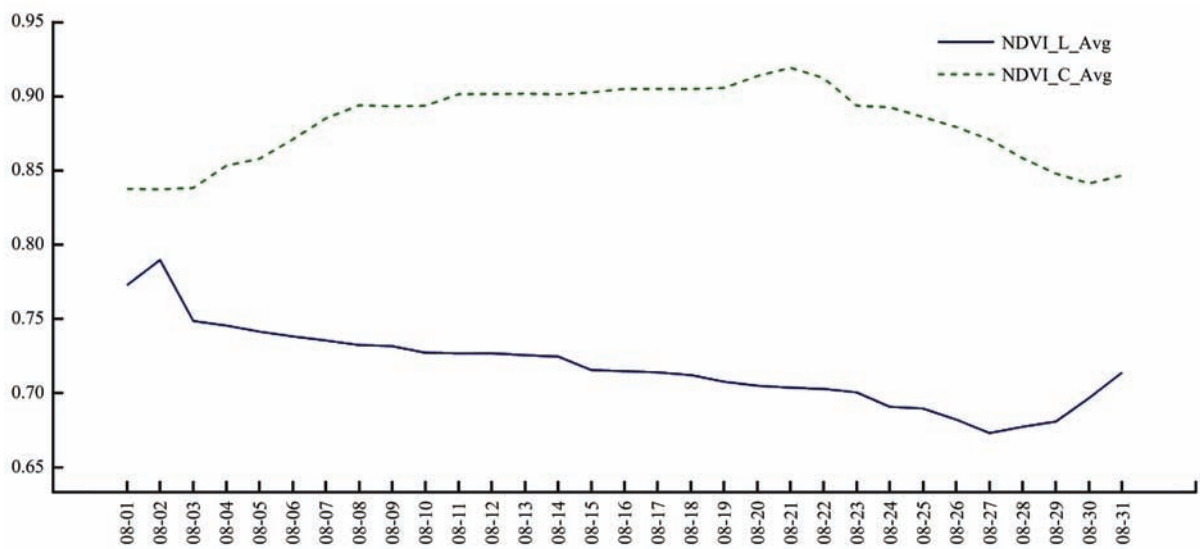
Note: y_L =leaf NDVI, x_C =canopy NDVI, x_D =growing days, x_{ETH} =highest temperature in environment, x_{CTH} = highest temperature of canopy rice, x_{MTH} =highest temperature in middle.

Figure 5 graphs the time series of the leaf and canopy NDVIs in August. During the filling stage, the canopy NDVI data reached the highest level on August 20. After the beginning of the rapid decline, the leaf NDVI decreased, resulting mainly due to the filling stage, during which leaf nutrients are continuously transferred to the panicle.



Note: NDVI_L_Avg—rice leaf NDVI, NDVI_C_Avg— rice canopy NDVI.

Figure 4 Canopy NDVI and leaf NDVI of Shendao-47 time-series curve in jointing and booting stage (2015)



Note: NDVI_L_Avg—rice leaf NDVI, NDVI_C_Avg—rice canopy NDVI.

Figure 5 Canopy NDVI and leaf NDVI of Shendao-47 time-series curve entering grain-filling stage (2015)

3.2.4 Mature stage

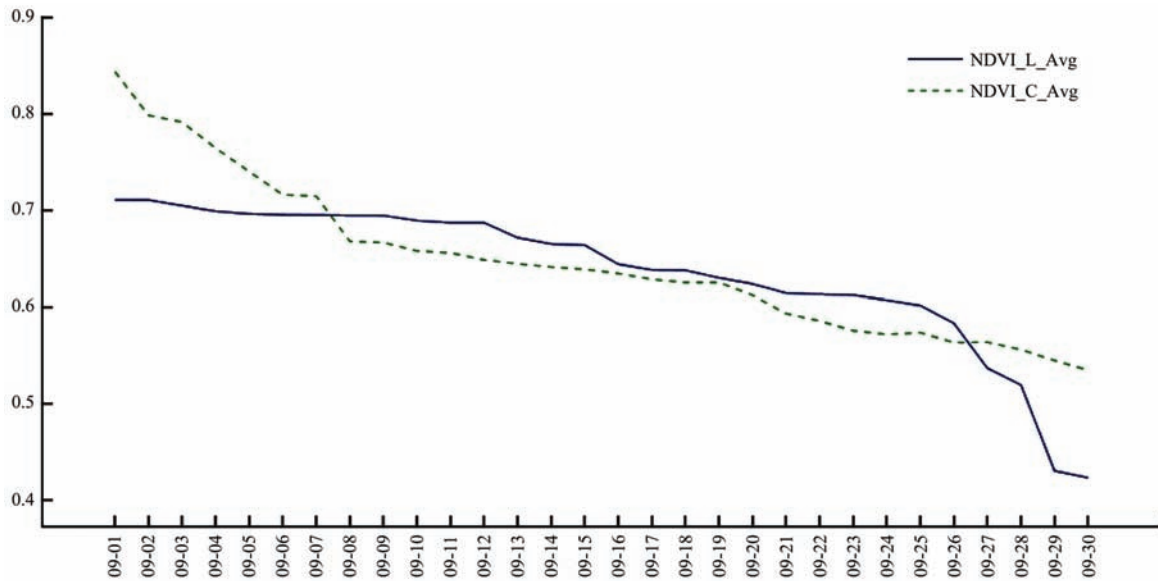
In September, the Shendao-47 reached maturity, the last stage of growth, during which the leaves turn yellow, the canopy and leaf NDVIs being very low and the yield basically formed. On the basis of the established model, this stage of the leaf NDVI fitting model was composed of the canopy NDVI, the duration of sunshine, and the number of days. The leaf NDVI is not related to the changes in temperature and humidity, which also means that changes in the environmental temperature and humidity did not influence the final output (Table 6).

Table 6 Leaf NDVI modeling and analysis of different environmental parameters in mature stage

Regression model	R ²
$y_L = -0.705 - 1.056x_C - 0.009x_D + 0.176x_S$	0.903
$y_L = 1.227 + 0.424x_C + 0.011x_{CTA} + 0.176x_{MTH}$	0.612
$y_L = 0.215 + 0.043x_C - 0.094x_{MTL} + 0.116x_{BTL}$	0.553

Note: y_L =leaf NDVI, x_C =canopy NDVI, x_D =growing days, x_{CTA} =average temperature of canopy rice, x_{MTH} =highest temperature in middle, x_{MTL} =lowest temperature in middle, x_{BTL} =lowest temperature in bottom.

As shown in Figure 6, in the mature stage, both NDVIs decreased and the canopy NDVI decreased significantly. After the second intersection, the leaf NDVI declined rapidly, which indicating that the rice was ripe.



Note: NDVI_L_Avg—rice leaf NDVI, NDVI_C_Avg—rice canopy NDVI.

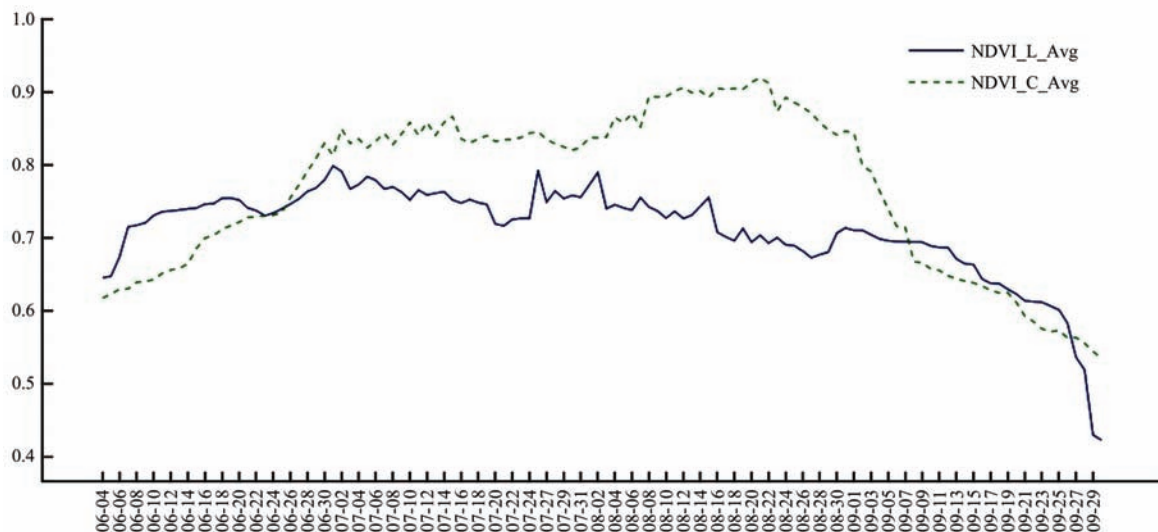
Figure 6 Canopy NDVI and leaf NDVI of Shendao-47 time-series curve in mature stage (2015)

3.3 Time-series analysis

Figure 7 shows the time-series curves for the leaf and canopy NDVIs of Shendao-47 from transplanting to maturity.

Three intersection points exist on the time-series curves of the leaf and canopy NDVIs, the first point being on June 27, 2015. Before this period, the leaf NDVI was higher than the canopy NDVI because the LAI was small. The canopy NDVI also contained most of the water layer. At this time, the leaves grew rapidly; therefore, the canopy NDVI was smaller than the leaf NDVI during this period. After this period of LAI growth, the canopy NDVI was greater than the leaf NDVI; hence the two curves at the first intersection represent a sign of growth and the tillering stage^[36]. The second

intersection of the two curves occurred on September 8, 2015. Before this date, the canopy NDVI was greater than the leaf NDVI. The leaf NDVI was greater than canopy the NDVI after this date because of the continuous growth of the leaves and the stem energy being transferred to the panicle. This phenomenon caused the leaves to turn yellow, this time for the dough-stage node. The third point of the two curves of intersection occurred on September 27, 2015. Beyond this point, the leaf NDVI rapidly decreased because the rice was essentially mature, and more than 90% of the leaves had become yellow^[37]. Therefore, predicting the key growth process of the rice became possible by using the time-series curves to graph the canopy and leaf NDVIs (Table 7).



Note: NDVI_L_Avg—rice leaf NDVI, NDVI_C_Avg—rice canopy NDVI.

Figure 7 Canopy NDVI and leaf NDVI of Shendao-47 time-series curves (2015)

Table 7 Use of canopy and leaf NDVIs to predict key growth period of japonica rice (Traditional time is approximate time range)

Prediction time	NDVIs	Period	Traditional time
2015/6/26	Canopy NDVI was greater than leaf NDVI	Tillering stage	2015/6/25
2015/7/1	Leaf NDVI maximum	Jointing stage	2015/7/1–2015/07/05
2015/7/21	Maximum difference between NDVIs in July	Booting stage	2015/7/25
2015/8/2	Minimum difference between NDVIs in August	Initial heading stage	2015/8/5
2015/8/22	Maximum difference between NDVIs	Milk stage	2015/8/24
2015/9/8	Leaf NDVI was greater than NDVI	Dough stage	2015/9/3
2015/9/27	Canopy NDVI was greater than leaf NDVI in September	Maturity	2015/10/1

3.4 Discussion

This study analyzed the relationship between the canopy and leaf NDVI scales of japonica rice. In a 2013 study the USDA suggested that the crop and leaf canopies of the same vegetation index have different sensitivities, and this kind of difference affects the accuracy of crop information inversions^[38]. The results of this study indicate that the respective scales of the NDVIs for different growth periods of rice canopies and leaves are different, thereby corroborating the results of previous research. The changes in the leaf NDVI during the growth cycle were much less than the changes in the canopy NDVI; however, after the filling stage, the changes in both NDVIs were relatively small. Although a rapid change in the leaf NDVI was caused by the transfer of leaf energy to the grain, a phenomenon that could reflect a change in the final stage of the crop, it has been the focus of fewer problems in previous research on rice NDVI. This research focused mainly on the process of establishing a model while taking into account the environmental factors and canopy NDVI. The results indicate that the influence of different parts of rice on the NDVI is different, by means of the canopy NDVI and environmental data detection to obtain the leaf NDVI value. However, this study did not take into account the influence of soil conditions on the model. Furthermore, some previous experience is a prerequisite for obtaining such a model. Moreover, additional research is needed in the future for further promotion of the model in future studies, especially from the perspective of a mechanism to further explain the relationships between the leaves and canopy NDVIs.

4 Conclusions

Our studies conducted in Northeast China have

demonstrated that the leaf NDVI of japonica rice can be simulated by the canopy NDVI and environmental data. The main contributions of this research are as follows: (1) Four periods of leaf NDVI models were established with good accuracy ($R^2=0.782-0.903$) that can predict the key stages in the rice growth period; (2) The collected canopy NDVI combining with environmental data can obtain the leaf NDVI information more efficiently, which cannot realize with traditional canopy remote sensing; (3) The results demonstrated that rice leaf NDVIs are influenced by environmental factors and canopy NDVIs. Therefore, leaf NDVIs can be estimated by canopy NDVIs and multisource environmental data that may be used for rice growth management.

Acknowledgments

The authors gratefully acknowledge that this research was supported by a grant from the national key research and development plan of China (2016YFD02006 00) and the EcoLab laboratory for allowing us to use their instruments.

[References]

- [1] Xue L H, Li G H, Qin X, Yang L Z, Zhang H L. Topdressing nitrogen recommendation for early rice with an active sensor in south China. *Precision Agriculture* 2014; 15(1): 95–110.
- [2] Chen C F, Son N T, Chang L Y. Monitoring of rice cropping intensity in the upper mekong delta, vietnam using time-series MODIS data. *Advances in Space Research* 2012; 49(2): 292–301.
- [3] Zheng L, Zhu D Z, Liang D, Zhang B H, Wang C, Zhao C J. Winter wheat biomass estimation based on canopy spectra. *Int J Agric & Biol Eng*, 2015; 8(6): 30–36.
- [4] Gebhardt S, Huth J, Nguyen LD, Roth A, Kuenzer C. A comparison of TerraSAR-X quadpol backscattering with

- RapidEye multispectral vegetation indices over rice fields in the mekong delta, vietnam. *International Journal of Remote Sensing*, 2012; 33(24): 7644–7661.
- [5] Zhang Z T, Lan Y, Wu P T, Han W T. Model of soybean NDVI change based on time series. *Int J Agric & Biol Eng*, 2014; 7(5): 64–70.
- [6] Gnyp M L, Miao Y, Yuan F, Ustin S L, Yu K, Yao Y, et al. Hyperspectral canopy sensing of paddy rice aboveground biomass at different growth stages. *Field Crops Research*, 2014, 155(155): 42–55.
- [7] Huang W J, Huang J F, Wang X Z, Wang F M, Shi J J. Comparability of red/near-infrared reflectance and NDVI based on the spectral response function between MODIS and 30 other satellite sensors using rice canopy spectra. *Sensors*, 2013; 13(12): 16023–16050.
- [8] Liu K L, Liu X, Hui H U, Duan H X, Xia G. Diagnosis of growth status of regenerated rice based on NDVI-value of main rice at key growth stage. *Acta Agriculturae Jiangxi*, 2015; 27(02): 7–11. (in Chinese with English abstract)
- [9] Huang J, Wang H M, Dai Q, Han D W. Analysis of NDVI data for crop identification and yield estimation. *IEEE Journal of Selected Topics in Applied Earth Observations and Remote Sensing* 2014; 7(11): 4374–4384.
- [10] Onoyama H, Ryu C, Suguri M, Iida M. Nitrogen prediction model of rice plant at panicle initiation stage using ground-based hyperspectral imaging: growing degree-days integrated model. *Precision Agriculture*, 2015; 16(5): 558–570.
- [11] Pan Z K, Huang J F, Zhou Q B, Wang L M, Cheng Y X, Zhang H K, Blackburn G A, Yan J, Liu J H. Mapping crop phenology using NDVI time-series derived from HJ-1 A/B data. *International Journal of Applied Earth Observation and Geoinformation*, 2015; 34: 188–197.
- [12] Wang P, Lan Y B, Luo X W, Zhou Z Y, Wang Z G, Wang Y H. Integrated sensor system for monitoring rice growth conditions based on unmanned ground vehicle system. *Int J Agric & Biol Eng*, 2014; 7(2): 75–81.
- [13] García D I, White W N. Control design of an unmanned hovercraft for agricultural applications. *Int J Agric & Biol Eng*, 2015; 8(2): 72–79.
- [14] Wang H S, Chen J S, Wu Z F, Lin H. Rice heading date retrieval based on multi-temporal MODIS data and polynomial fitting. *International Journal of Remote Sensing*, 2012; 33(6): 1905–1916.
- [15] Wu B F, Gommers R, Zhang M, Zeng H W, Yan N N, Zou W T, et al. Global crop monitoring: a satellite-based hierarchical approach. *Remote Sensing*, 2015; 7(4): 3907–3933.
- [16] Yao X, Ren H, Cao Z, Tian Y, Cao W, Zhu Y, et al. Detecting leaf nitrogen content in wheat with canopy hyperspectrum under different soil backgrounds. *International Journal of Applied Earth Observation and Geoinformation*, 2014; 32: 114–124.
- [17] Zhang Z, Song X, Chen Y, Wang P, Wei X, Tao F L. Dynamic variability of the heading-flowering stages of single rice in China based on field observations and NDVI estimations. *International Journal of Biometeorology*, 2015; 59(5): 643–655.
- [18] Shibayama M, Sakamoto T, Takada E, Inoue A, Morita K, Yamaguchi T, Takahashi W, Kimura A. Estimating rice leaf greenness (SPAD) using fixed-point continuous observations of visible red and near infrared narrow-band digital images. *Plant Production Science*, 2012; 15(4): 293–309.
- [19] Sun H, Li M Z, Zhang Y N, Zheng L H, Zhang Y J. Correlation between chlorophyll content and vegetation index of maize plants under different fertilizer treatments with multi-spectral imaging. *Sensor Letters*, 2013; 11(6-7): 1128–1133.
- [20] Camacho F, Cernicharo J, Lacaze R, Baret, F, Weiss, M. GEOV1: LAI, FAPAR essential climate variables and FCOVER global time series capitalizing over existing products. Part 2: Validation and intercomparison with reference products. *Remote Sensing of Environment*, 2013; 137(10): 310–329.
- [21] Verónica C, Anatoly G, James S. Non-destructive determination of maize leaf and canopy chlorophyll content. *Journal of Plant Physiology*, 2009; 166(2):157–167.
- [22] Manjunath K R, More R S, Jain N K, Panigrahy S, Parihar J. S. Mapping of rice-cropping pattern and cultural type using remote-sensing and ancillary data: a case study for south and southeast asian countries. *International Journal of Remote Sensing*, 2015, 36(24): 6008–6030.
- [23] Liu K L, Li Y Z, Hu H W. Predicting ratoon rice growth rhythm based on NDVI at key growth stages of main rice. *Chilean Journal of Agricultural Research*, 2015, 75(4): 410–417..
- [24] Roberge V, Tarbouchi M, Labonte G. Comparison of parallel genetic algorithm and particle swarm optimization for real-time uav path planning. *IEEE Transactions on Industrial Informatics*, 2013; 9(1): 132–141.
- [25] Gutierrez M. Effect of leaf and spike morphological traits on the relationship between spectral reflectance indices and yield in wheat. *International Journal of Remote Sensing*, 2015, 36(3): 701–718.
- [26] Macbean N, Maignan F, Peylin P, Bacour C, Bréon F M, Ciais P. Using satellite data to improve the leaf phenology of a global terrestrial biosphere model. *Biogeosciences Discussions*, 2015; 12(12): 13311–13373.
- [27] Acerbi Júnior F W, Silveira E M D O, Mello J M D, Mello C R D, Scolforo J R S. Change detection in Brazilian

- savannas using semivariograms derived from NDVI images. *Ciência E Agrotecnologia*, 2015; 39(2): 103–109.
- [28] Hirooka Y, Homma K, Maki M, Sekiguchi K. Applicability of synthetic aperture radar (SAR) to evaluate leaf area index (LAI) and its growth rate of rice in farmers' fields in Lao PDR. *Field Crops Research*, 2015, 176: 119–122.
- [29] Liebisch F, Kirchgessner N, Schneider D, Walter A, Hund A. Remote aerial phenotyping of maize traits with a mobile multi-sensor approach. *Plant Methods*, 2015, 11(1): 1–20.
- [30] Mishra N B, Chaudhuri G. Spatio-temporal analysis of trends in seasonal vegetation productivity across Uttarakhand, Indian Himalayas, 2000–2014. *Applied Geography*, 2015, 56: 29–41.
- [31] Xie Q, Huang W, Zhang B, Chen P. Estimating winter wheat leaf area index from ground and hyperspectral observations using vegetation indices. *IEEE Journal of Selected Topics in Applied Earth Observations & Remote Sensing*, 2015, 9(2): 1–10.
- [32] Li X, Yu B, Xin L, Min T, Shi H. Canopy NDVI analysis and yield estimation for cotton in different nitrogen treatments. *Transactions of the Chinese Society for Agricultural Machinery*, 2014, 45(7): 231–236. (in Chinese with English abstract)
- [33] Rahman M M, Lamb D W, Stanley J N. The impact of solar illumination angle when using active optical sensing of NDVI to infer fAPAR in a pasture canopy. *Agricultural & Forest Meteorology*, 2015, 202(202): 39–43.
- [34] Gitelson A A, Peng Y, Huemmrich K F. Relationship between fraction of radiation absorbed by photosynthesizing maize and soybean canopies and NDVI from remotely sensed data taken at close range and from MODIS 250m resolution data. *Remote Sensing of Environment*, 2014, 147(10): 108–120.
- [35] Li W, Saphores J D M, Gillespie T W. A comparison of the economic benefits of urban green spaces estimated with NDVI and with high-resolution land cover data. *Landscape & Urban Planning*, 2015, 133: 105–117.
- [36] Tubana B, Harrell D, Walker T, Teboh J, Lofton J, Kanke Y, et al. Relationships of spectral vegetation indices with rice biomass and grain yield at different sensor view angles. *Agronomy Journal*, 2011; 103(5): 1405–1413.
- [37] Huang J F, Wang X Z, Li X X, Tian H Q, Pan Z K. Remotely sensed rice yield prediction using multi-temporal NDVI data derived from NOAA's-AVHRR. *Plos One*, 2013; 8(8): e70816–e7081.
- [38] Hunt E R, Doraiswamy P C, McMurtrey J E, Daughtry C S T, Perry E M, Akhmedov B. A visible band index for remote sensing leaf chlorophyll content at the canopy scale. *International Journal of Applied Earth Observation & Geoinformation*, 2013; 21(4): 103–112.